

# Reversible Insertion of Iridium into a Cyclopropenyl Carbon-Carbon Bond

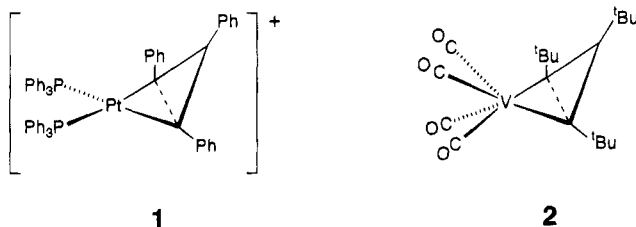
Russell P. Hughes,<sup>\*,1a</sup> David S. Tucker,<sup>1a</sup> and Arnold L. Rheingold<sup>1b</sup>

Departments of Chemistry, Burke Chemistry Laboratory, Dartmouth College, Hanover, New Hampshire 03755-3564, and University of Delaware, Newark, Delaware 19716

Received July 27, 1994<sup>®</sup>

**Summary:** Decarbonylation of the cyclopropenyl-iridium complex **3** affords the dinuclear complex **4**, in which both cyclopropenyl rings remain intact. Further decarbonylation of **4** yields the crystallographically characterized dinuclear complex **5** in which both rings have been ruptured, one to give a bridging C<sub>3</sub> ligand and one to give a terminal C<sub>3</sub> ligand. The latter ligand represents a structure intermediate between a cyclopropenyl (metallatetrahedrane) complex and a metallacyclobutadiene, illustrating an *insertio interrupta* of iridium into a carbon-carbon bond. Complex **5** is fluxional on the NMR time scale, with interconversion of the two *tert*-butyl environments for the terminal C<sub>3</sub> ligand. It also reacts rapidly with CO to re-form the metallatetrahedrane complex **3**, demonstrating quantitative reversibility of the insertion process.

The valence isomeric relationship between  $\eta^3$ -cyclopropenyl complexes (metallatetrahedranes) and metallacyclobutadienes has been recognized as significant in alkyne metathesis,<sup>2</sup> and the energy surface for this isomerization has been mapped theoretically.<sup>3</sup> While almost all transition-metal complexes with cyclopropenyl ligands exhibit the expected options of  $\eta^3$  or  $\eta^1$  ligation,<sup>4</sup> two examples of " $\eta^2$ -cyclopropenyl" ligands have been reported in which the metal-C<sub>3</sub> interactions lie at points intermediate between metallacyclobutadiene and tetrahedrane structures, as defined by the distance *R* and the angle  $\phi$  shown in Figure 1. In platinum complex **1**  $\phi = 111^\circ$  and  $R = 1.58(2) \text{ \AA}$ ,<sup>5</sup> while the more recently reported vanadium complex **2** has  $\phi = 106.9^\circ$  and  $R = 1.710(11) \text{ \AA}$ ,<sup>6</sup> in each case the bond



between the two ligated carbon atoms is clearly rather weak. These two complexes represent points on the energy surface between an  $\eta^3$ -cyclopropenyl ligand and

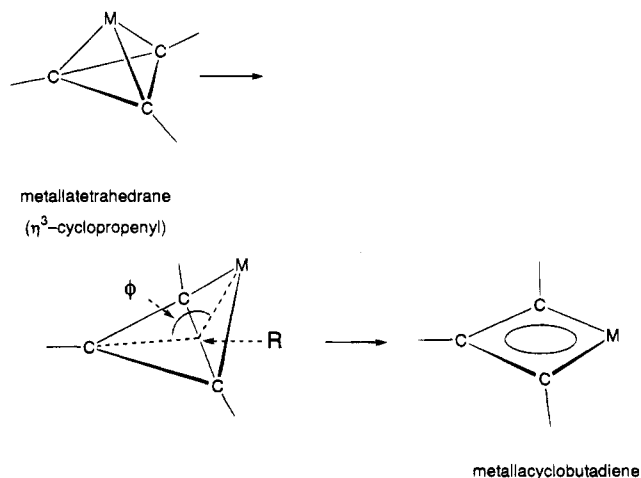


**Figure 1.** Conversion of a metallatetrahedrane ( $\eta^3$ -cyclopropenyl) complex to a metallacyclobutadiene complex via an intermediate structure.  $\phi$  is the dihedral angle between the M-C-C and C-C-C planes; *R* is the distance between the two ligated carbon atoms in the intermediate.

a planar metallacyclobutadiene and delineate a partial insertion (*insertio interrupta* (i.i.)) of the metal into the C-C bond. They differ from the few examples of "puckered metallacyclobutadiene" complexes<sup>7</sup> in that the latter exhibit localized single and double bonding within the ring and between the metal and the two carbon atoms. In contrast, **1** and **2** exhibit a more symmetrical interaction of the metal with the carbon framework and contain an approximate plane of symmetry passing through the metal atom and the distal carbon of the C<sub>3</sub> unit.<sup>5,6</sup> Here we report a third such complex which lies even further along this i.i. pathway, in which the C-C bond of the ligand has been stretched well beyond a reasonable bonding distance.

We have shown previously that the ( $\eta^3$ -cyclopropenyl)-iridium complex **3**<sup>8</sup> undergoes decarbonylation on reaction with *N*-methylmorpholine *N*-oxide (NMO) in the presence of olefins and alkynes (L) to give the complexes  $[\text{Ir}(\eta^3\text{-C}_3^t\text{Bu}_3)(\text{CO})\text{L}]$ .<sup>9</sup> In the absence of added ligands this decarbonylation reaction affords the red dinuclear complex **4**<sup>10</sup> in which the two cyclopropenyl rings remain intact. The structure of **4** has been confirmed crystallographically and will be reported elsewhere.<sup>11</sup> Further reaction of **4** with NMO results in decomposition, but gentle heating in dichloromethane solution results in loss of another molecule of CO and formation of the red

<sup>®</sup> Abstract published in *Advance ACS Abstracts*, November 1, 1994.

(1) (a) Dartmouth College. (b) University of Delaware.

(2) Schrock, R. R. *Acc. Chem. Res.* **1986**, *19*, 342.

(3) Jemmis, E. D.; Hoffmann, R. *J. Am. Chem. Soc.* **1980**, *102*, 2570. See also: Lin, Z.; Hall, M. B. *Organometallics* **1994**, *13*, 2878.

(4) See: Shen, J.-K.; Tucker, D. S.; Basolo, F.; Hughes, R. P. *J. Am. Chem. Soc.* **1993**, *115*, 11312. Lichtenberger, D.; Hoppe, M. L.; Subramanian, L.; Kober, E. M.; Hughes, R. P.; Hubbard, J. L.; Tucker, D. S. *Organometallics* **1993**, *12*, 2025 and references therein.

(5) McClure, M. D.; Weaver, D. L. *J. Organomet. Chem.* **1973**, *54*, C59.

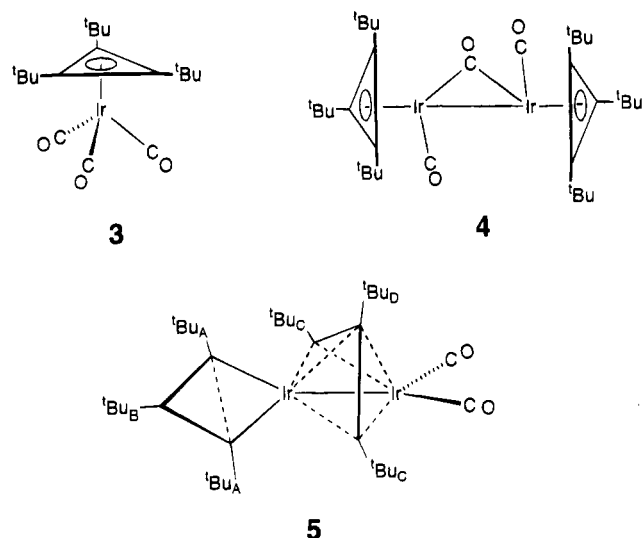
(6) Blunden, R. B.; Cloke, F. G. N.; Hitchcock, P. B.; Scott, P. *Organometallics* **1994**, *13*, 2917.

(7) Weinstock, I. A.; Schrock, R. R.; Davis, W. M. *J. Am. Chem. Soc.* **1991**, *113*, 135 and references therein. Churchill, M. R.; Ziller, J. W.; McCullough, L.; Pedersen, S. F.; Schrock, R. R. *Organometallics* **1983**, *2*, 1046.

(8) Hughes, R. P.; Tucker, D. S.; Rheingold, A. L. *Organometallics* **1993**, *12*, 3069.

(9) Hughes, R. P.; Tucker, D. S. *Organometallics* **1993**, *12*, 4736.

dinuclear complex **5**.<sup>12</sup> The crystallographically deter-



mined structure of **5** is shown as an ORTEP diagram in Figure 2, along with some key bond distances and angles; details of the crystallographic determination are provided in Table 1.<sup>13</sup> The Ir(1)–Ir(2) distance of 2.842(1) Å is consistent with a single bond between the two metal centers. The structure is remarkable in that both of the original cyclopropenyl rings have been ruptured; one C<sub>3</sub> ligand is bridging and the other is terminal. The  $\mu$ -C<sub>3</sub>tBu<sub>3</sub> ligand is analogous to similar bridging units found elsewhere.<sup>14</sup> In particular, the distance C(1)–

(10) NMO (0.44 g, 3.7 mmol) was added to a THF (30 mL) solution of **3** (1.80 g, 3.7 mmol). This mixture was cooled to –30 °C and stirred overnight. After solvent removal *in vacuo* (and without filtering) the deep red solid product was chromatographed on an alumina column (3 × 25 cm, –70 °C), first with hexanes as eluent (400 mL) followed by diethyl ether (100 mL). The first fraction contained unreacted **3** (0.98 g, 2.0 mmol, 54%) and the second fraction contained **4** (0.72 g, 0.82 mmol, 44%), which yielded red needles from hexanes. Mp: 141–143 °C dec. IR (hexanes):  $\nu_{\text{CO}}$  1982, 1954, 1931, 1844, 1830 cm<sup>-1</sup>. <sup>1</sup>H NMR (CDCl<sub>3</sub>):  $\delta$  1.25 (s), <sup>13</sup>C{<sup>1</sup>H} NMR (CDCl<sub>3</sub>):  $\delta$  196.28 (CO), 73.07 (C<sub>3</sub>tBu<sub>3</sub>), 30.68 (CH<sub>3</sub>), 29.92 (CMe<sub>3</sub>). Anal. Calcd for C<sub>33</sub>H<sub>54</sub>Ir<sub>2</sub>O<sub>3</sub>: C, 44.88; H, 6.16; Found: C, 44.99; H, 6.00. Changing the mole ratio of NMO to **3** does not afford higher yields.

(11) Rheingold, A. L. Unpublished results.

(12) A CH<sub>2</sub>Cl<sub>2</sub> (15 mL) solution of **4** (0.110 g, 0.125 mmol) was heated to reflux for 23 h. After solvent removal *in vacuo*, the red-orange solid product was chromatographed on a Florisil column (1 × 20 cm, –70 °C), first with hexanes as eluent (600 mL) followed by diethyl ether (60 mL). The first fraction contained **3** (0.069 g, 0.142 mmol, 57%), and the second fraction contained **5** (0.039 g, 0.046 mmol, 36%). Red plates of **5** were afforded by recrystallization from hexanes. Mp: 172 °C dec. IR (hexanes):  $\nu_{\text{CO}}$  2002, 1938 cm<sup>-1</sup>. <sup>1</sup>H NMR (CDCl<sub>3</sub>; 20 °C):  $\delta$  1.70 (s, 18H, tBu<sub>C</sub>), 1.39 (s, br, 27H, tBu<sub>A,B</sub>), 1.18 (s, 9H, tBu<sub>D</sub>). <sup>13</sup>C{<sup>1</sup>H} NMR (toluene-*d*<sub>6</sub>, –80 °C):  $\delta$  188.66 (CO), 166.70, 118.93, 44.94, 32.38 (C<sub>3</sub>tBu<sub>3</sub>), 33.03 (CH<sub>3</sub>), 32.50 (CH<sub>3</sub>), 30.47 (CH<sub>3</sub>), 29.67 (CH<sub>3</sub>), 41.72 (CMe<sub>3</sub>), 38.53 (CMe<sub>3</sub>), 37.17 (CMe<sub>3</sub>), 33.32 (CMe<sub>3</sub>). Anal. Calcd for C<sub>32</sub>H<sub>54</sub>Ir<sub>2</sub>O<sub>2</sub>: C, 44.94; H, 6.36; Found: C, 45.21; H, 6.06.

(13) Crystals of **5** were obtained from diethyl ether. Preliminary photographic characterization showed that **5** possessed *mmm* symmetry. Systematic absences in the diffraction data uniquely established the space group as *Pbca*. Data were empirically corrected for absorption using 216 data (6 reflections, 10° increments). The structure was solved by direct methods and completed by difference Fourier synthesis. All non-hydrogen atoms were refined with anisotropic thermal parameters. All hydrogen atoms were treated as idealized, updated isotropic contributions. Computations were made with the *SHELXTL PLUS* (4.27) program library (G. Sheldrick, Siemens, Madison, WI).

(14) Bailey, P. M.; Keasey, A.; Maitlis, P. M. *J. Chem. Soc., Dalton Trans.* **1978**, 1825–1830. Keasey, A.; Maitlis, P. M. *J. Chem. Soc., Dalton Trans.* **1978**, 1830–1839. Frisch, P. D.; Posey, R. G.; Khare, G. P. *Inorg. Chem.* **1978**, *17*, 402–408. Hoberg, H.; Krause-Going, R.; Kruger, C.; Sekutowski, J. C. *Angew. Chem., Int. Ed. Engl.* **1977**, *16*, 183–184. Chisholm, M. H.; Jansen, R.-M.; Huffman, J. C. *Organometallics* **1992**, *11*, 2305–2307. Chisholm, M. H.; Heppert, J. A.; Huffman, J. C. *J. Am. Chem. Soc.* **1984**, *106*, 1151–1153.

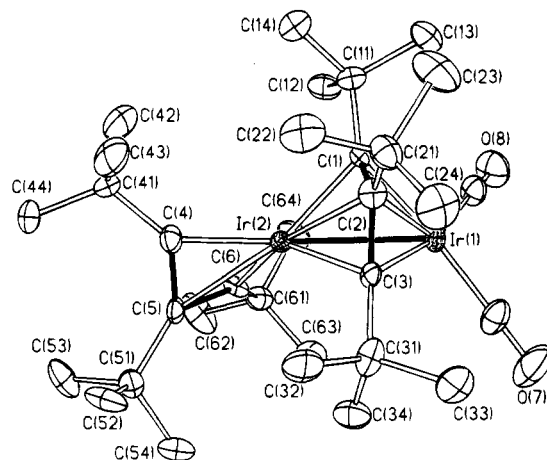


**Figure 2.** Molecular structure of **5** drawn with 35% probability ellipsoids. Selected bond distances (Å): Ir(1)–Ir(2), 2.842(1); Ir(1)–C(1), 2.115(12); Ir(1)–C(2), 2.437(14); Ir(1)–C(3), 2.093(12); Ir(1)–C(7), 1.842(18); Ir(1)–C(8), 1.879(15); Ir(2)–C(1), 2.072(13); Ir(2)–C(2), 2.408(14); Ir(2)–C(3), 2.071(13); Ir(2)–C(4), 2.004(14); Ir(2)–C(5), 2.430(13); Ir(2)–C(6), 1.964(12); C(1)–C(2), 1.492(19); C(2)–C(3), 1.454(19); C(4)–C(5), 1.420(21); C(5)–C(6), 1.432(18); C(4)–C(6), 1.995(19). Selected bond angles (deg): C(1)–C(2)–C(3), 136.2(12); C(1)–C(2)–C(3), 100.9(11); C(1)–C(2)–C(21), 129.3(12); C(3)–C(2)–C(21), 129.8(12); Ir(2)–C(4)–C(5), 88.7(9); C(4)–C(5)–C(6), 88.8(11).

**Table 1. Crystal Data for 5**

(a) Crystal Parameters	
formula	C <sub>32</sub> H <sub>54</sub> Ir <sub>2</sub> O <sub>2</sub>
cryst syst	orthorhombic
space group	<i>Pbca</i>
<i>a</i> , Å	16.891(4)
<i>b</i> , Å	18.492(4)
<i>c</i> , Å	20.662(7)
<i>V</i> , Å <sup>3</sup>	6454(2)
<i>Z</i>	8
<i>D</i> (calc), g cm <sup>-3</sup>	1.760
$\mu$ (Mo K $\alpha$ ), cm <sup>-1</sup>	82.33
temp, K	296
cryst size, mm	0.30 × 0.30 × 0.40
cryst color	dark red
(b) Data Collection	
diffractometer	Nicolet R3m/ $\mu$
monochromator	oriented graphite
radiation	Mo K $\alpha$
wavelength, Å	0.710 73
2 $\theta$ limits, deg	4 < 2 $\theta$ < 50
std rflns	3 std/197 rflns
decay, %	~2
octants colled	+ <i>h</i> , + <i>k</i> , <i>l</i>
no. of rflns colled	6258
no. of indep rflns	5669
no. of indep rflns, $F_o > 3\sigma(F_o)$	3273 ( $F_o \geq 5\sigma(F_o)$ )
<i>T</i> (max)/ <i>T</i> (min)	1.70
(c) Refinement	
<i>R</i> ( <i>F</i> ), %	4.08
<i>R</i> <sub>w</sub> ( <i>F</i> ), %	4.67
GOF	0.93
$\Delta\sigma$ (max)	0.001
$\Delta(\rho)$ , e Å <sup>-3</sup>	1.01
<i>N</i> <sub>o</sub> / <i>N</i> <sub>v</sub>	10.0

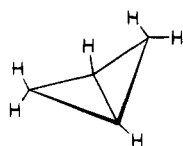
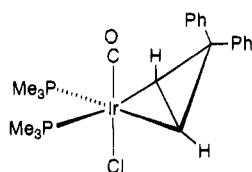
C(3) of 2.27 Å indicates complete rupture of the C–C bond. The terminal C<sub>3</sub>tBu<sub>3</sub> ligand is similar to that found in complex **2**.<sup>6</sup> The geometry at C(5) is planar with a long Ir(2)–C(5) distance of 2.430(13) Å, indicating little Ir–C interaction, whereas the Ir(2)–C(4) and Ir(2)–C(6) distances of 2.004(14) and 1.964(12) Å are essentially equivalent, and the two *tert*-butyl groups on these carbon atoms are bent back from the plane of the

**Table 2.** Values of  $\phi$  and  $R$  for **1**, **2**, and **5–7**

compd	$\phi$ (deg) <sup>a</sup>	$R$ (Å) <sup>a</sup>
<b>1</b>	111	1.58
<b>2</b>	106.9	1.710
<b>5</b>	123.5	1.995
<b>6</b>	126.0	1.53
<b>7</b>	126.3	1.45

<sup>a</sup> See Figure 1 for definitions of  $\phi$  and  $R$ .

C(4)–C(5)–C(6) unit by 30.1 and 26.6°, respectively, indicating strong metal interaction with these two carbon atoms. There is no evidence of localized bonding between the carbons of the C<sub>3</sub> unit, with the distances C(4)–C(5) (1.420(21) Å) and C(5)–C(6) (1.432(18) Å) being equal within experimental error. Notably, the degree of insertion of Ir(2) into the C(4)–C(6) bond is significantly more advanced than that observed for vanadium in **2** or platinum in **1**. Comparisons of the dimensions  $R$  and  $\phi$  for **1**, **2**, and **5** are provided in Table 2, along with analogous parameters for bicyclo[1.1.0]butane (**6**)<sup>15</sup> and an  $\eta^2$ -cyclopropene complex of Ir (**7**).<sup>16</sup>

**6****7**

The angle  $\phi$  for **5** (123.5°) is significantly larger than those observed for **1** or **2** but quite similar to those in **6** and **7**. The distance  $R$  for **5** (1.995(14) Å) is incompatible with any significant bonding between the two carbon atoms.

In compounds **1** and **2** the crystallographically determined C<sub>s</sub> structures exhibited fluxional behavior in which all three carbon atoms involved in the M–C<sub>3</sub> interaction are equivalent even at low temperatures on the NMR time scale.<sup>5,6</sup> Similar behavior is observed for the terminal C<sub>3</sub> ligand in **5**; at room temperature this ligand exhibits only one broad resonance for *t*-Bu<sub>A,B</sub> by <sup>1</sup>H NMR, which becomes a sharp singlet at 80 °C and which decoalesces into two resonances of ratio 2:1 at –50 °C. Line shape analysis of the variable-temperature spectra affords  $\Delta G^\ddagger = 58$  kJ mol<sup>–1</sup> for the process causing interconversion between *t*-Bu environments A and B in the terminal ligand. The simplest mechanism for this interconversion involves closure of the ring, cyclopropenyl rotation, and reopening along another C–C bond. We assume that the apparently higher

activation barrier for this process in **5** compared to that in **1** and **2** arises because the iridium is further inserted into the C–C bond in the ground state, leading to a higher barrier for the ring closure step.<sup>17</sup>

The two inequivalent *t*-Bu resonances C and D of the  $\mu$ -C<sub>3</sub><sup>t</sup>Bu<sub>3</sub> ligand do not coalesce, nor is there observable exchange between the bridging and terminal C<sub>3</sub><sup>t</sup>Bu<sub>3</sub> ligands. However, the *t*-Bu groups C in the bridging ligand do decoalesce below room temperature and at –85 °C appear as three peaks of equal intensity, presumably due to hindered rotation about the *t*-Bu–C single bond. This decoalescence is not observed in the low-temperature <sup>13</sup>C NMR spectrum, perhaps due to similar chemical shifts. Analysis of the variable-temperature <sup>1</sup>H NMR spectra affords  $\Delta G^\ddagger = 45$  kJ mol<sup>–1</sup> for this process, a value not unlike the  $\Delta G^\ddagger = 39$  kJ mol<sup>–1</sup> for *tert*-butyl rotation in 2,2,3,3-tetramethylpentane.<sup>18</sup>

Extrusion of Ir from both these C–C bonds is extremely facile. Treatment of a red solution of **5** with CO results in rapid bleaching of the color and quantitative regeneration of monomeric **3**. The driving force for re-formation of the three-membered rings presumably arises from release of steric interactions between adjacent *t*-Bu groups. We cannot distinguish whether this reverse reaction proceeds via **4**, as this complex too reacts extremely rapidly with CO to afford **3**.

These results indicate that, under appropriate conditions, insertion of late transition metals into C–C bonds can be facile and reversible. Further chemistry of **5** is being explored.

**Acknowledgment.** R.P.H. is grateful to the National Science Foundation for generous financial support. A loan of iridium chloride from Johnson Matthey Aesar/Alfa is gratefully acknowledged. We thank F. G. N. Cloke and P. Scott (University of Sussex) and R. H. Grubbs (California Institute of Technology) for sharing results prior to their publication.

**Supplementary Material Available:** Tables giving a structure determination summary, atomic coordinates and equivalent isotropic displacement coefficients, bond lengths, bond angles, anisotropic displacement coefficients, and H-atom coordinates and isotropic displacement coefficients for **5** (10 pages). Ordering information is given on any current mast-head page.

OM940598H

(17) This mechanism cannot be distinguished from one involving further opening of the ring to form a metallacyclobutadiene, which can interconvert the two environments via equilibrium with an alkylidyne (alkyne) complex in which the alkyne can rotate. We prefer our suggestion, because the higher activation barrier observed for this process in **5** is consistent with closure of the ring being important.

(18) Bushweller, C. H.; Anderson, W. G.; Goldberg, M. J.; Gabriel, M. W.; Gilliom, L. R.; Mislow, K. *J. Org. Chem.* **1980**, *45*, 3880.

(15) Haller, I.; Srinivasan, R. *J. Chem. Phys.* **1964**, *41*, 2745.

(16) Li, R. T.; Nguyen, S. T.; Grubbs, R. H.; Ziller, J. W. *J. Am. Chem. Soc.*, in press.